Crystallization, melting and morphology of syndiotactic polypropylene fractions: 2. Linear crystal growth rate and crystal morphology

Jonahira Rodriguez-Arnold, Zhengzheng Bu and Stephen Z. D. Cheng*
Maurice Morton Institute and Department of Polymer Science, The University of Akron, Akron, OH 44325-3909, USA

and Eric T. Hsieh, Tim W. Johnson, Rolf G. Geerts, Syriac J. Palackal, Gil R. Hawley and M. Bruce Welch
Research and Development, Phillips Petroleum Company, Bartlesville, OK 74004, USA
(Received 25 April 1994)

Linear crystal growth rates of two narrow molecular weight fractions of syndiotactic polypropylene having the same syndiotacticity have been measured using polarized light microscopy over a temperature range of >20°C. It has been found that a regime III to regime II transition at a supercooling of ~50°C exists. Structure analysis via electron diffraction (ED) experiments indicates that no change of growth planes has been found during this regime transition. Nevertheless, a gradual change of the crystal perfection due to a chain packing change from a crystal incorporated with isochiral packing defects to a majority of cell III structure in this supercooling range has been observed. The validity of the nucleation theory applied to s-PP is discussed. For the crystal morphological study, single crystals with rectangularly faceted lamellae can be grown at high crystallization temperatures (low supercooling) in thin s-PP film samples as observed via transmission electron microscopy. Similar to the results reported by Lovinger and Lotz, the ED patterns show that the long axis of the single lamellar crystal is the *b*-axis. On decreasing the crystallization temperature, spherulites are developed. Cracks on the lamellar crystals have been observed, and they are always perpendicular to the *b*-axis. This phenomenon has been explained by invoking the observation that the coefficient of thermal expansion along the *b*-axis is about one order of magnitude larger than that along the *a*-axis, as measured via wide-angle X-ray diffraction experiments. However, at high crystallization temperatures, the cracks are found less frequently. This is due to the pure cell III crystal packing that forms at these tempratures leading to the incorporation of fewer isochiral packing defects which promote crack initiation.

(Keywords: linear crystal growth rate; morphology; syndiotactic polypropylene)

INTRODUCTION

The discovery of stereospecific polymerization allowed for the first time steric control on the growth of polymer chains. Isotactic polypropylene (i-PP) has received much attention over the years since it was first commercialized in 1958. In the years following the initial synthesis of the isotactic form, Natta and co-workers successfully synthesized and characterized the syndiotactic form of polypropylene (s-PP)[1,2]. More recently, new metallocene catalysts based on zirconium (Zr) and hafnium (Hf) have been developed[3], and much higher syndiotacticity in s-PP is achieved.

The possibility of the s-PP chain existing in three different conformations leads to the observed polymorphism. The crystal structure in a s-PP sample critically depends on the crystallization conditions such as the supercooling, crystallization/annealing time, the chain stereoregularity and sequence, and the molecular weight and molecular weight distribution. The high temperature orthorhombic form of s-PP is the most stable crystal form. There are four monomer units per translational repeat unit with a binary symmetry axis perpendicular to the helix axis and passing through the CH_2 groups. The chain has an $S(2/1)2$ symmetry corresponding to a $(t_2g_2)_2$ conformation. The unit cell was initially proposed[1] to be orthorhombic with $a = 1.450$ nm and $b = 0.580$ nm (later, it was found that $b = 0.560$ nm)[4], c(chain axis) $= 0.740$ nm, $\alpha = \beta = \gamma = 90°$ and space group $C222_1$. This symmetry, as determined by Natta's group, was based on the systematic absence of $h + k = 2n + 1$ reflections in the wide-angle X-ray diffraction (WAXD) fibre patterns.

In the late 1980s, Lotz *et al.* observed additional reflections and streaks through electron diffraction (ED) of single lamellar crystals in thin films of s-PP[5-8]. The presence of $h + k = 2n + 1$ reflections which have not been seen on the fibre patterns studied previously were clearly identified. Moreover, these reflections are forbidden for a unit cell with a space group $C222_1$. As a consequence,

*To whom correspondence should be addressed

0032-3861/94/24/5194–08

a different symmetry is necessary for unit cell II which has the same dimensions as unit cell I. In this case helices of alternating handedness are incorporated along the *a*-axis resulting in a unit cell face-centred on the *ac* plane with a space group $Pca2_1$. Furthermore, based on the reflections in the ED of single crystals obtained by isothermal crystallization at higher temperatures, an orthorhombic unit cell III, was ultimately proposed with $a = 1.450$ nm, $b = 1.120$ nm, $c = 0.740$ nm, and a space group of *Ibca*. Unit cell II was then recognized as a strong subcell of unit cell III. The 'doubling' of the original unit cell I along the *b*-axis is a consequence of the different packing. Incorporation of both left- and right-handed helices is allowed in the lattice along both the *a*- and *b*-axes. The alternation of left- and right-handed helices is known as antichiral packing, which is required by unit cell III[5-8]. It should be noted that the existence of the separate unit cell I is still strongly defended by De Rosa and Corradini via their study in the annealed s-PP WAXD fibre patterns[9].

Besides the high temperature orthorhombic form, a low temperature orthorhombic form with a relatively stable form consisting of planar zigzag polymer chains was also observed with $a = 0.522$ nm, $b = 1.117$ nm, c (chain axis) $= 0.506$ nm with a space group of *C2cm*[10]. Chatani *et al.*[11] reported a new triclinic cell with a space group *P1*, with $a = 0.572$ nm, $b = 0.764$ nm, c (chain axis) $= 1.160$ nm, $\alpha = 73.1°$, $\beta = 88.8°$, $\gamma = 112.0°$.

The crystal morphology of s-PP has not received much attention in the last 30 years and only two papers have been published[7,12]. Marchetti and Martuscelli studied the morphology of solution grown single crystals of s-PP in various solvents and the effects of chain defects and thermal history on the crystal morphology. The sample with the highest stereoregularity was the only one that showed elongated single crystals with irregular edges. The crystallographic facet was proposed to be along the longitudinal direction of the single crystals. They also suggested that most likely the fold planes were the 100 and the 110 of cell I (cells II and III were not recognized at that time) and that the growth direction may be coincident with both the *a*- and the *b*-axes. Twinned monolayer crystals were also found which are believed to develop from defective nuclei[12]. Attempts to obtain ED patterns failed due to the extremely short-lived reflections. Samples with lower syndio-regularity exhibited dendritic-like textures. Long spacing measurements by small-angle X-ray scattering (SAXS) and the corresponding deduced lamellar thicknesses showed a decrease with decreasing syndiotacticity.

Lovinger *et al.*[7] have studied the crystal morphology of s-PP crystals grown from the melt in the thin films and its dependence on supercooling. Samples used possess a *racemic* dyad content of 0.769 and syndiotactic and isotactic triads of 0.698 and 0.159, respectively. At the lowest supercoolings (the highest crystallization temperatures, T_cs $> 105°C$), large, rectangular, faceted lamellar crystals were observed by phase-contrast light microscopy and transmission electron microscopy (TEM). Based on the ED patterns, these crystals had the same unit cell and interchain packing consistent with cell III. At a high supercooling ($T_c = 90°C$), twinned crystals seem to be more common. As T_c was further lowered, the morphology became axialitic and eventually spherulitic ($T_c = \sim 60°C$). ED patterns with increasing streaking along the $\langle h20 \rangle$ reflections (cell III) suggested that with increasing supercooling the intermolecular packing along the *a*-axis systematically deviates from the regular antichiral form due to kinetic reasons during crystallization. More specifically, the packing disorder, as described previously, was believed to be introduced along the *b*-axis with the incorporation of isochiral chains. Overgrowth observed by TEM on the s-PP crystals grown from samples of relatively low syndiotacticity were identified as individual i-PP crystals.

The overall crystallization kinetics of s-PP has also been studied. Balbontin *et al.*[13] studied the overall crystallization kinetics in fractions of s-PP with varying syndiotacticities and molecular weights. They reported values for the Avrami exponent n between 1.8 and 3.7. Similarly, the kinetic constant K was determined as having values between 0.16×10^{-3} and 4.77×10^{-3}, depending on the percentage of *racemic* dyads and molecular weight. Very recently, we have reported the study of overall crystallization kinetics on a series of s-PP fractions with different molecular weights, but the same syndiotacticities, and similar results have been found[14].

Only one publication has reported studies on the linear crystal growth rate kinetics of s-PP[15]. In that study the spherulitic growth of a s-PP sample having 72% syndiotacticity in an isothermal T_c range of 40°C ($97.4°C < T_c < 137.3°C$) was measured. Using equilibrium values of $T_m^\circ = 161°C$, $\Delta h_f^\circ = 3.14\ \text{kJ mol}^{-1}$ and assuming regime II growth, the lateral and fold surface free energies, σ and σ_e, were estimated to be 4.4 and 47 erg cm^{-2}, respectively. The work of chain folding (q) was 23.4 kJ mol^{-1}. It was also noted that the growth rate data of s-PP is of the same order of magnitude as i-PP for similar degrees of supercooling.

In 1984 Clark and Hoffman fitted the growth rate data of Miller and Seeley with a straight line for temperatures above 110°C[16]. They suspected a break in the curve below this temperature which would lead to regime III (at $\Delta T = \sim 50°C$). Because of the lack of data at the corresponding temperatures this could not be confirmed. Clark and Hoffman estimated $\sigma_e = 49.9\ \text{erg cm}^{-2}$ and $q = 24.3\ \text{kJ mol}^{-1}$.

Morphological changes corresponding to crystallization in a specific regime have been investigated for several polymers. In polyethylene, spherulitic structures are observed at intermediate supercoolings, namely, regime II. At the transition between regimes II/I a gradual change in the sign and magnitude of the birefringence, and axialitic morphologies are observed[17,18]. In poly-(pivalolactone), a gradual change from spherulitic to axialitic is observed at the regime III/II transition[19]. In i-PP, no correlation between morphological changes and regime transitions was observed[20]. One additional argument made recently by Point *et al.* was that in the vicinity of the regime III/II transition, a change of crytallographic planes along the crystal growth front (parallel to the radial direction of the spherulites) was observed in poly(ethylene oxide) fractions via a microbeam WAXD experiment[21]. They concluded that the crystal growth rate change is not a surface nucleation mechanism change but rather a change of the growth front plane.

EXPERIMENTAL

Materials

The s-PP fractions used in this study were supplied by Phillips Petroleum Company (Bartlesville, OK). A

Table 1 Molecular characterization of s-PP fractions

Sample	$M_n(\times 10^3)$	$M_w(\times 10^3)$	M_w/M_n	[r](%)[a]	[rr](%)[b]	[rrr](%)[c]	r-Block[d]
s-PP(3)	20.8	22.9	1.1	95	93	88	37.8
s-PP(5)	33.3	36.6	1.1	94	92	86	34.1
s-PP(8)	76.8	84.5	1.1	94	92	86	31.7
s-PP(9)	132.0	158.4	1.2	95	92	87	33.9
s-PP(10)	234.0	280.0	1.2	95	92	87	34.1

[a] *Racemic* conformation [*r*]
[b] Triads [*rr*]
[c] Pentads [*rrrr*]
[d] Number-averaged syndiotactic block, 2([*rr*] + [*mr*]/2)/[*mr*]

detailed molecular analysis has been reported in the first part of this series[14]. Two of the s-PP fractions were studied. Their molecular characteristics are given in *Table 1*. Thin films ($\sim 10\ \mu$m thick) were prepared for polarized light microscopy (PLM) observations. The samples prepared for TEM were obtained from solution cast films having a thickness of $<0.2\ \mu$m.

In reality, it is extremely difficult to achieve a 100% stereoregular tacticity as mistakes are introduced into the chain molecules. Two kinds of mistakes with respect to isotacticity may be identified for i-PP. The first is caused by catalysts in which two consecutive *racemic* conformations [*rr*] are needed to correct the mistake. The second type is called end-chain mistake since only one *racemic* conformation [*r*] is needed, followed by a change of D- to L-helices or vice versa. The tacticity mistakes in s-PP should be illustrated in a similar way, but in this case, these two types of mistakes should possess [*mm*] and [*m*] configurations. The number of mistakes (defects), as well as the distribution of these defects, then affect the crystal structure and the crystallization process. The number and nature of chain defects will also affect the thermodynamic and mechanical properties of the polymer.

Instrumentation and experiments

Crystal growth rates were measured via PLM (Olympus HB-2) coupled with a Mettler FP-82 hot stage. Isothermal crystallization experiments were conducted at different temperatures for each fraction. The thin film samples were heated to 180°C for 2 min in another hot stage and then they were quickly switched to the hot stage which possesses a preset isothermal temperature. Since the growth rates in these s-PP fractions were very fast, ASA 1600 Kodak films were used for continuously quick exposures in order to obtain a precise measure of the growth rates. Each picture had an exposure time of 2 s. After the film was developed, the growth rates were measured directly from the photographs. At each temperature, five independent measurements were carried out to ensure the reproducibility of the growth rate data.

Crystal morphology was observed via TEM (JEOL JEM-120U) with an accelerating voltage of 120 kV. The ultra thin films were also isothermally crystallized at different temperatures using the same procedure described in the PLM experiments. After complete crystallization, the films were cooled to room temperature. The film samples were then subjected to conventional Pt–C shadowing and carbon backing before being transferred to copper grids.

WAXD experiments were carried out on a Rigaku 12 kW rotating anode as the X-ray source. Powder

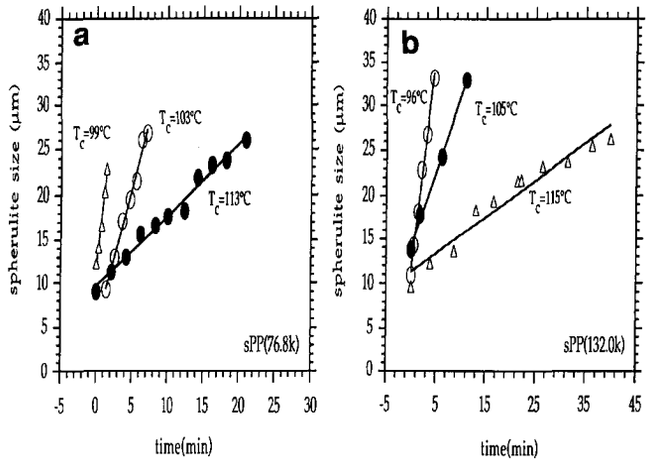

Figure 1 Relationships between the spherulitic growing size and time for s-PP fractions with molecular weight of (a) 76.8×10^3 and (b) 132.0×10^3 isothermally crystallized at three different temperatures

samples were prepared and were isothermally crystallized at different temperatures in a hot stage on the X-ray diffractometer. Careful measurements of the positions of the (200) and (020) reflection peaks were carried out at different temperatures. The slope of a specific peak position change with temperature represents the coefficient of thermal expansion of the corresponding crystalline plane.

RESULTS AND DISCUSSION

Linear crystal growth rates and regime transitions

As described in the previous section, the linear crystal growth rates of the s-PP fractions can only be measured via photographs. *Figure 1* shows the spherulitic size changes with time at different isothermal T_cs for two s-PP fractions with intermediate to high molecular weights (76.8×10^3 and 132.0×10^3). Linear relationships are clearly found. The slopes of these linear lines are thus the crystal growth rates of the s-PP fractions at different temperatures. *Figure 2* shows a series of PLM micrographs to illustrate the spherulitic morphology of the s-PP crystals on which the linear growth rates were measured. If one plots the relationship between the logarithmic linear crystal growth rates and supercooling as shown in *Figure 3*, a general trend of decreasing rates with decreasing supercooling (increasing isothermal T_c) is evident. A clear feature is that a discontinuity of the growth rates appears at $\Delta T = \sim 50$°C ($T_c = 110$°C) for both s-PP fractions. This is a first implication that a possible regime transition in the crystal growth may exist.

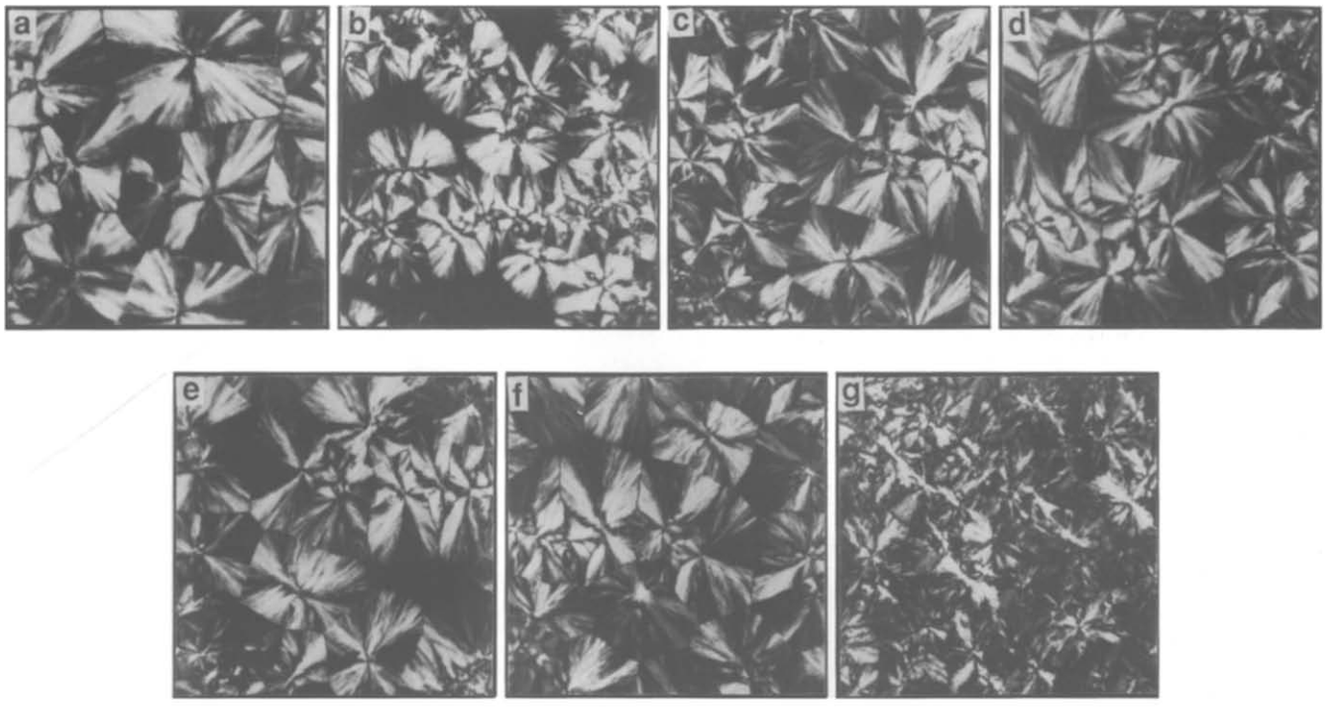

Figure 2 Spherulitic texture observed via PLM for s-PP ($MW = 132.0 \times 10^3$) at different isothermal temperatures: (a) 101; (b) 106; (c) 107; (d) 109; (e) 111; (f) 113; (g) 117°C

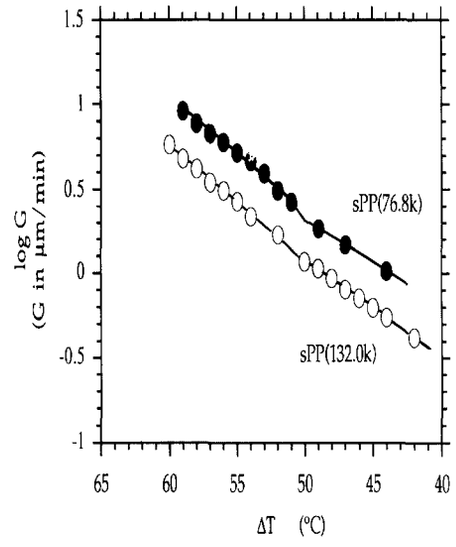

Figure 3 Relationships between logarithmic linear growth rates and supercooling for two s-PP fractions

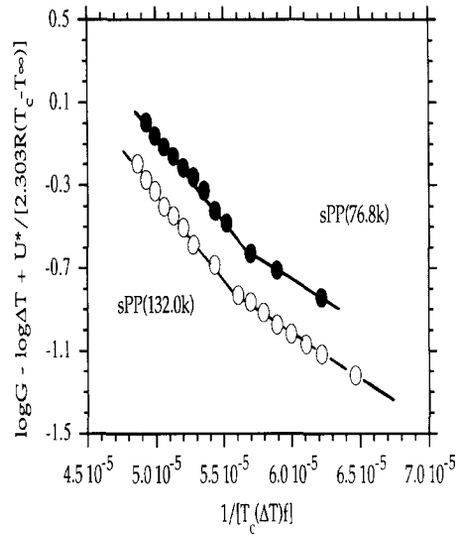

Figure 4 Nucleation theory treatment of the linear growth rate data for two s-PP fractions

When one utilizes the nucleation theory[17,18,22–27] to treat the growth rate data, a plot of $\log G - \log \Delta T + U^*/[2.303R(T_c - T_\infty)]$ *versus* $1/[T_c(\Delta T)f]$ must be constructed based on the nucleation theory:

$$G = G_0(\Delta T)\exp\{-U^*/[R(T_c - T_\infty)]\} \times \exp\{-K_g/[T_c(\Delta T)f]\} \quad (1)$$

which defines the linear crystal growth rate G of polymer crystals in each regime based on the theory[17,18,22–27]. The parameter K_g is also known as the nucleation constant and contains the contributions from the surface free energies. The existence of different regimes is confirmed by a change of the slope in the plots based on equation (1). From *Figure 4*, a clear regime III to regime II transition can be observed. In this treatment, the equilibrium melting temperature of 160°C is used based on our observation reported previously[14], and a universal activation energy term is applied (6.28 kJ mol^{-1})[22]. The slopes are listed in *Table 2*. It can be seen that the ratio of two neighbouring slopes is close to two as predicted by the theory[17,18,22–27]. Furthermore, based on the equilibrium heat of fusion[14] of 8.0 kJ mol^{-1}, the product of the lateral and fold surface free energies, $\sigma\sigma_e$, is found to lie in the range of 465–538 erg^2 cm^{-4} (*Table 2*). Since the lateral surface free energy is calculated to be $\sim$11 erg cm^{-2} based on the equation:

$$\sigma = (0.1)\Delta h_f^\circ (a_0 b_0)^{0.5} \quad (2)$$

where $a_0 b_0$ is a cross-sectional area of one chain molecule, the fold surface free energies of these two fractions in different regimes can be calculated as listed in *Table 2*.

Table 2 Nucleation theory parameters based on linear crystal growth data for two s-PP fractions

Sample	$K_g(\times 10^5)(K^{-2})$	$\sigma\sigma_e(erg^2\,cm^{-4})$	$\sigma_e(erg\,cm^{-2})$	$q(kJ\,mol^{-1})$	Ratio[a]
Regime II					
s-PP(8)	0.9433	474	42	21	2.0
s-PP(9)	1.060	537	47	23	1.9
Regime III					
s-PP(8)	1.856	466	42	20	
s-PP(9)	1.975	500	44	22	

[a]The ratio between two neighbouring regimes is given by $K_g(III)/K_g(II)$

They are between 42 erg cm^{-2} and 47 erg cm^{-2}. The fold energy can thus be obtained at ~20–24 kJ mol^{-1}. These calculated fold surface free energies can also be confirmed by comparing with those calculated through the slopes of the relationship between the melting temperature and lamellar thickness[14] (~45 erg cm^{-2}). Both the lateral and fold surface free energies are smaller than those in the case of i-PP[20].

The regime III to regime II transition occurs at a supercooling near 50°C. This fits very well with the prediction proposed by Clark and Hoffman[16] which was based on the limited linear growth rate data in regime II reported by Miller and Seeley[15]. They reported that this regime transition should happen at a supercooling of ~50°C. However, other factors such as a change of growth front planes, a change of crystal forms, etc., may also cause this growth rate discontinuity. In s-PP, it has been known that there is a gradual perfection of the crystal from a chain packing incorporated with isochiral packing defects at low T_cs to an almost pure cell III structure crystallized at high tempratures as was discovered using WAXD and ED experiments[5–8,14]. This temperature range over which this happens is between 100°C and 120°C for these two s-PP fractions (see below), while the regime transition occurs at ~110°C. First, is this regime transition a gradual change of the slope in *Figure 4*? The answer is that this transition seems to be a relatively sharp one. Secondly, is this transition caused by the change of the unit cell in the crystal lattice? One has to carefully recognize the nature of this unit cell change with temperature. It has been reported that the change of unit cell with temperature is a kinetically controlled process[7]. Namely, at low T_cs, the crystal growth is relatively fast, and the chain molecules do not have enough time to arrange themselves to form a perfect cell III structure. Note that the cell III structure requires complete antichiral packing with opposite helical handedness along both the *a*- and the *b*-axes. A shift of half the distance along the *c*-axis is also necessary assuming the crystal growth is along the *b*-axis. As a result, at relatively low T_cs the restriction of chain conformations able to enter the crystal lattice is relatively low. It is possible for both right- and left-handed helices to be incorporated in the growth of the crystals. On increasing the T_c the crystal growth rate decreases, and the chain molecules have enough time to choose their lowest energy packing. Therefore, the most stable cell III packing is formed. If this explanation holds, one expects that a down-turn of the linear growth rate with increasing temperature should be found since the molecules need more time to carry out this perfect cell III packing. However, we observe an upturn of the linear growth rate with increasing temperature as shown in *Figures 3* and *4*. This indicates that the discontinuity in these growth rate data should not be the cause of the change of crystal lattice, but instead, a regime transition due to the change of surface nucleation mechanism is responsible.

In vinyl polymers such as i-PP and s-PP the molecular weight, tacticity and sequence distributions have effects on the crystallization kinetics, and therefore, on the regime transition analysis. The closest study towards s-PP considered the isotacticity effect was on a set of i-PP fractions with similar molecular weights (*MW*s) and molecular weight distributions[20]. The effect of different *MW*s on the crystallization kinetics and regime analysis of s-PP has been very recently reported for a set of s-PP fractions with the same syndiotacticity[14].

Crystal structure and morphology

In *Figure 2*, spherulitic texture of one s-PP fraction with $MW = 132.0 \times 10^3$ has been found under PLM in a 20°C supercooling range. Typical patterns of the Maltese cross extinctions are evident. With increasing temperature, the spherulitic texture becomes relatively coarse with irregular Maltese cross extinction. Further temperature increases lead to the growth of single lamellar crystals. All the s-PP fractions with *MW* of $>30 \times 10^3$ show similar spherulitic morphology. However, with increasing *MW*, single lamellar crystals are slightly more difficult to grow. We have thus chosen one fraction with $MW = 33.3 \times 10^3$ to investigate morphological changes with temperature. *Figure 5* shows a series of the ED patterns of s-PP single lamellar crystals crystallized at different temperatures. All of them possess a [00*l*] zone. It is evident that at the high temperature of 130°C (low ΔT of 30°C), sharp reflections are observed which can be indexed. This pattern indicates clearly a pure cell III lattice as proposed by Lotz and Lovinger and Lovinger *et al.*[5–8] Based on the space group $C222_1$, the 010 and 210 reflections should be forbidden, but they are found in the ED patterns in *Figure 5*. On decreasing the T_c, streaks are found along the $\langle h20\rangle$ reciprocal lines (cell III). As indicated by Lovinger *et al.*, these streaks represent the disorder caused by statistical departure from regular antichiral packing along the *b*-axis.

It is also important for the regime transition that no change in the crystal growth front plane occurs. *Figures 6* and *7* are TEM micrographs of the s-PP crystal morphology. At a T_c of 105°C, spherulitic texture is observed (*Figure 6*). On the other hand, a high T_c of 125°C leads to single lamellar crystals (*Figure 7*). The long axis is again along the *b*-axis. We have carefully examined the growth front plane in s-PP crystals between 105°C and 115°C; the *b*-axis is always found to be the preferred growing direction. As a result, we conclude that no growth

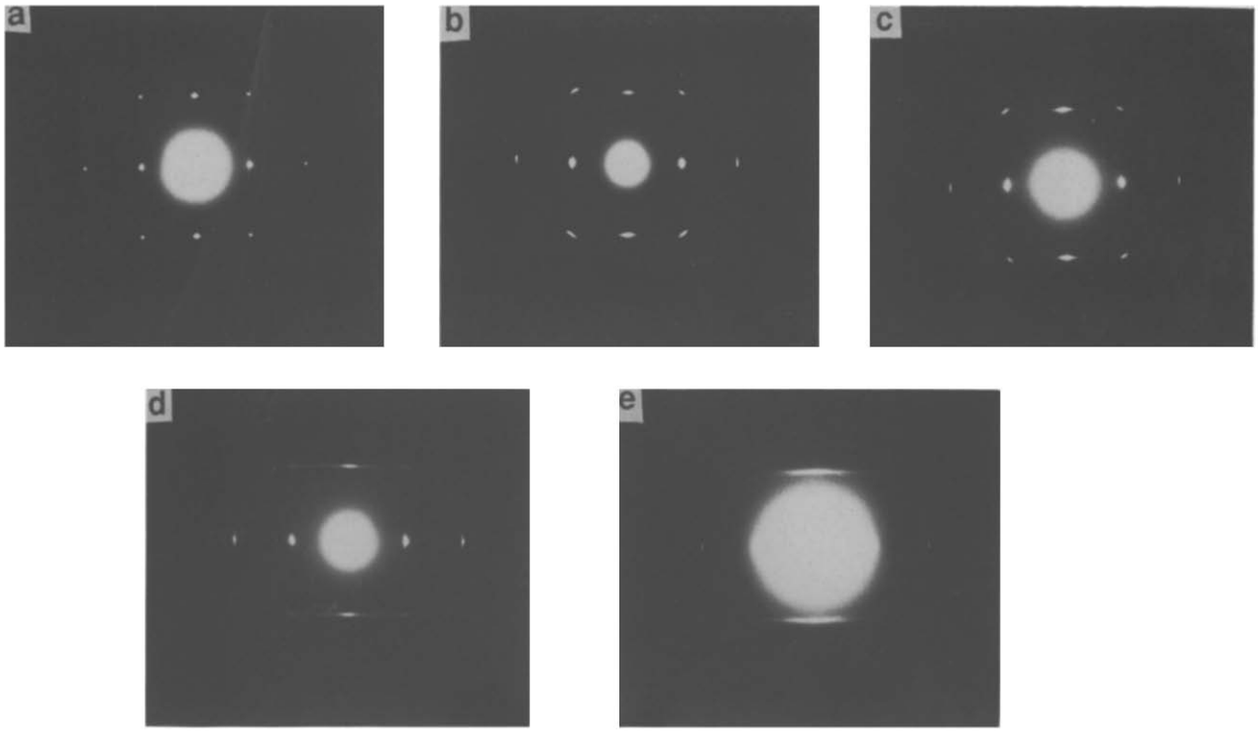

Figure 5 ED patterns of the single lamellar crystals for s-PP ($MW = 33.3 \times 10^3$) crystallized at different temperatures: (a) 130; (b) 120; (c) 110; (d) 100; (e) 90°C

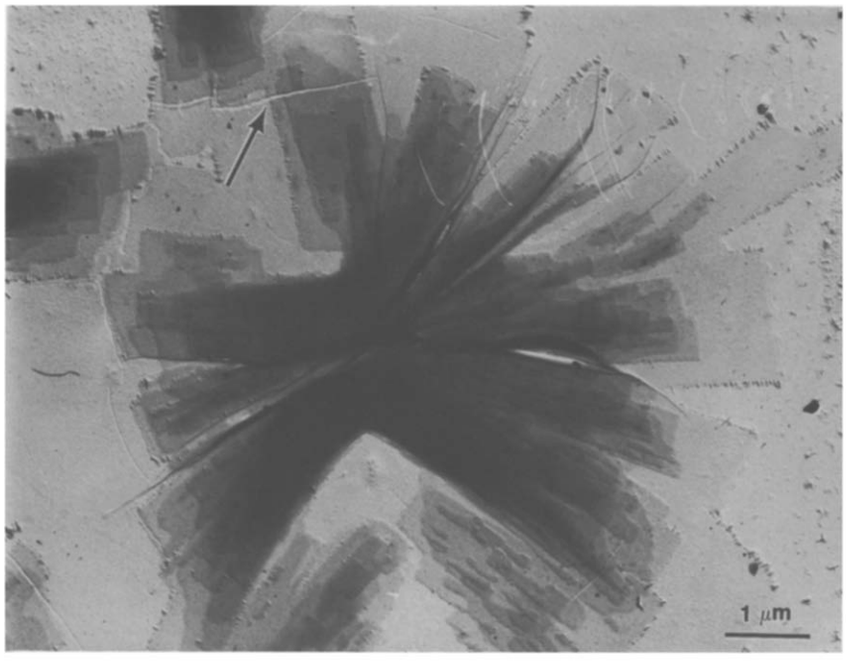

Figure 6 Spherulitic textures of s-PP fraction ($MW = 33.3 \times 10^3$) isothermally crystallized at 105°C

front plane change has been found during the regime transition.

Another interesting observation is the cracks found in the single crystals as shown in *Figures 6* and *8*. The cracks examined were always perpendicular to the *b*-axis. It was first pointed out to us by Lovinger that the coefficients of thermal expansion along the *a*- and *b*-axes are different as shown in *Figure 9* for both low and high *MW*s[8,28]. In fact, the coefficient of thermal expansion along the *b*-axis is about one order of magnitude higher than that along the *a*-axis ($2–3 \times 10^{-5}$ for the *a*-axis *versus* $2–3 \times 10^{-4}$ nm °C^{-1} for the *b*-axis). It is expected that these cracks may form when the lamellar crystals are cooled to room temperature after their isothermal crystallization. The difference of the coefficients of thermal expansion along both the *a*- and the *b*-axes can also be observed commonly in other polymer crystals, but the difference is more drastic in the case of s-PP compared with those other crystals. A very slight difference in the *a*- and *b*-axis dimensions between two fractions is also

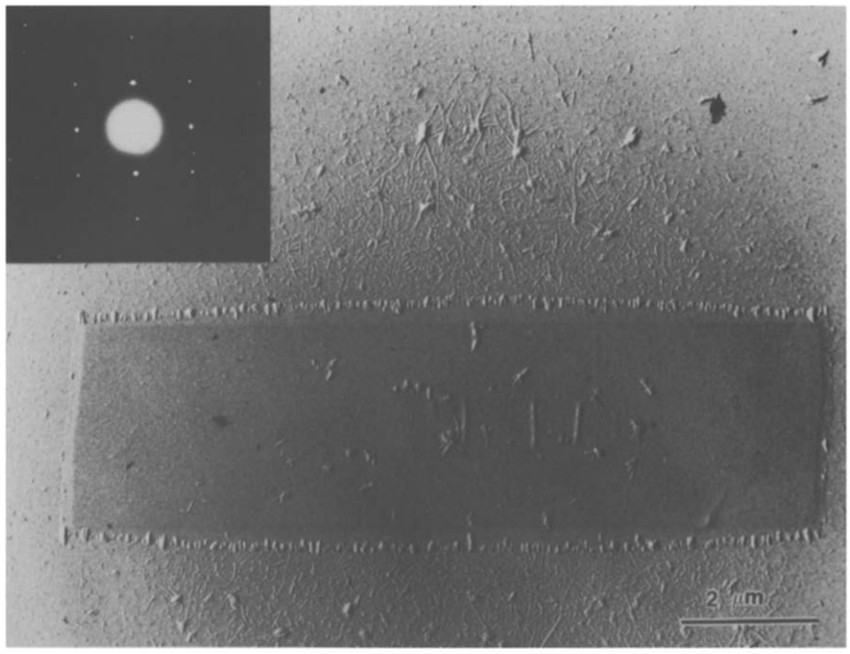

Figure 7 Single lamellar crystal of s-PP fraction ($MW = 33.3 \times 10^3$) isothermally crystallized at 125°C. The ED pattern is attached with proper orientation of the crystallographic axes

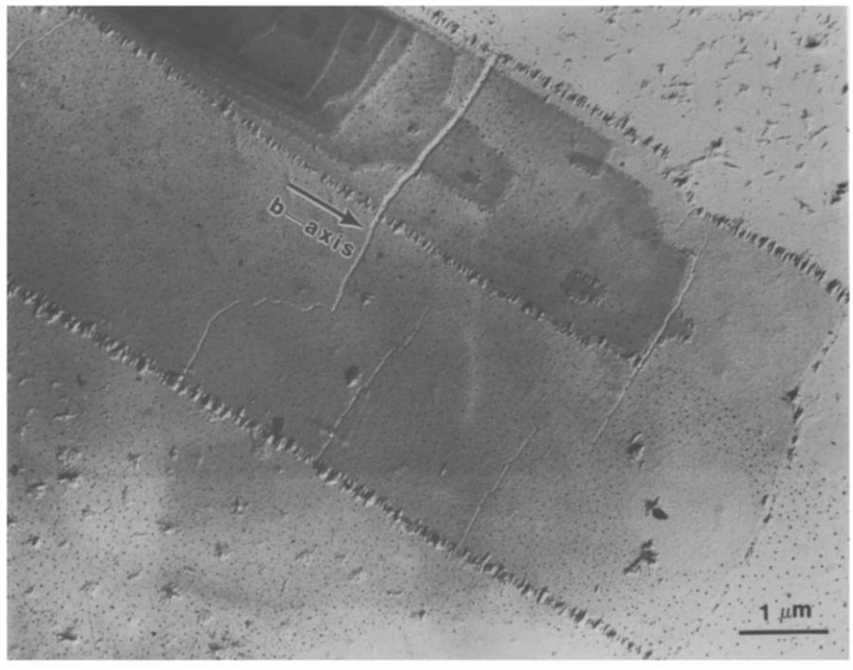

Figure 8 Single lamellar crystal of s-PP ($MW = 33.3 \times 10^3$) fraction with cracks perpendicular to the *b*-axis

seen. This may be the cause of the crystal lattice in the high MW fraction possessing a slightly higher lattice strain on the fold surfaces compared to that in the low MW fraction. This may lead to a lattice expansion for the crystals of the high MW fraction as observed. On the other hand, when the T_c is high enough, in our case it is >130°C, no cracks are found. We expect this may be due to the pure cell III crystal lattice formed above this temperature. Although the coefficients of thermal expansion along those two axes are very different, the initiation of the cracks must be from the aggregation of the defective packing structure of the s-PP crystals. Based on the computer modelling carried out by Lovinger *et al.*[8], at high temperatures the defects incorporated due to isochiral packing may travel to the growth front. There they will either be annihilated during the crystallization or else travel back into the crystal until they can aggregate adjacently to yield a macroscopic row defect which will construct a fault in the *ac* plane and form crystal fracture[8]. It is thus conceivable that the decrease of cracks in the crystals grown at high temperatures is due to a reduction of the number of isochiral packing defects and improved

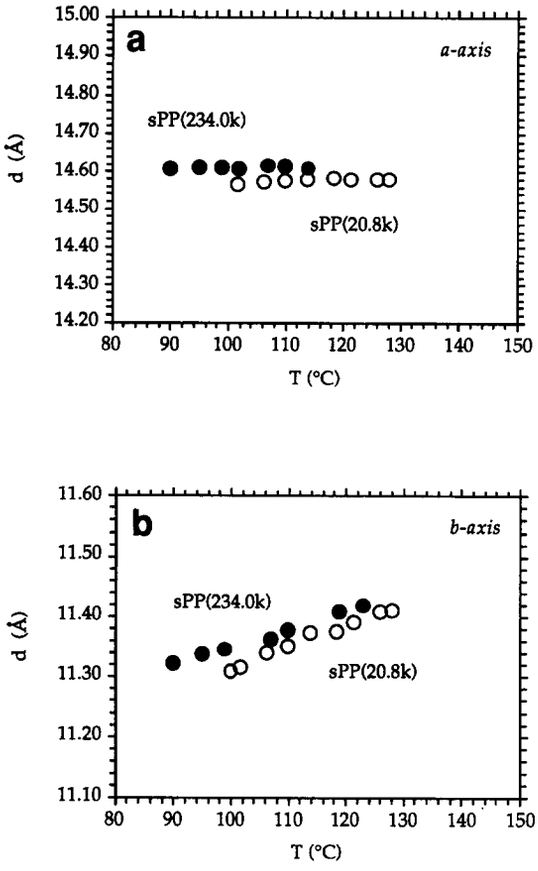

Figure 9 Coefficients of thermal expansion of the s-PP crystals along (a) the *a*-axis and (b) the *b*-axis measured via WAXD experiments for two s-PP fractions

perfection in the crystals. We thus conclude that both the large difference of the coefficients of thermal expansion and the defective crystal structure are the causes of crack formation in s-PP crystals.

CONCLUSIONS

We have observed a regime III to regime II transition in linear crystal growth rates of two s-PP fractions with intermediate to high *MW*s (76.8×10^3 and 132.0×10^3). This transition occurs at a supercooling of 50°C as predicted by Clark and Hoffman[16]. During the transition, the growth direction is always along the *b*-axis, and no change of the crystal growth front plane is found. It also seems that this transition cannot be explained by invoking the change of the crystal packing. The spherulitic morphology can be found at low T_cs, while single lamellar crystals are observed at high T_cs. The cracks found in the lamellar crystals are perpendicular to the *b*-axis, and can be attributed to the different coefficients of thermal expansion along both the *a*- and the *b*-axes as first proposed by Lovinger *et al.*[28,29], as well as the defective structures involved in the crystal lattice caused by isochiral chain packing.

ACKNOWLEDGEMENT

This research was supported by SZDC's Presidential Young Investigator Award from the National Science Foundation (DMR-9157738) and the indutrial matching funding provided by Phillips Petroleum Company.

REFERENCES

1 Natta, G., Pasquon, I., Corradini, P., Peraldo, M., Pegoraro, M. and Zambelli, A. *Rend. Acc. Naz. Lincei* 1960, **28**, 541
2 Natta, G., Pasquon, I. and Zambelli, A. *J. Am. Chem. Soc.* 1962, **84**, 1488
3 Ewen, J. A., Jones, R. L., Razavi, A. and Ferrara, J. D. *J. Am. Chem. Soc.* 1988, **110**, 6255
4 Corradini, P., Natta, G., Ganis, P. and Temussi, P. A. *J. Polym. Sci. C* 1967, **16**, 2477
5 Lotz, B., Lovinger, A. J. and Cais, R. E. *Macromolecules* 1988, **21**, 2374
6 Lovinger, A. J., Lotz, B. and Davis, D. *Polymer* 1990, **31**, 2253
7 Lovinger, A. J., Davis, D. and Lotz, B. *Macromolecules* 1991, **24**, 552
8 Lovinger, A. J., Lotz, B., Davis, D. and Padden Jr, F. J. *Macromolecules* 1993, **26**, 3494
9 De Rosa, C. and Corradini, P. *Macromolecules* 1993, **26**, 5711
10 Natta, G., Peraldo, M. and Allegra, G. *Makromol. Chem.* 1964, **75**, 215
11 Chatani, Y., Maruyama, H., Asanuma, T. and Shiomura, T. *J. Polym. Sci., Polym. Phys. Edn* 1991, **29**, 1649
12 Marchetti, A. and Martuscelli, E. *J. Polym. Sci. A2* 1974, **12**, 1649
13 Balbontin, G., Dainelli, D., Galimberti, M. and Paganetto, G. *Makromol. Chem.* 1993, **193**, 693
14 Rodriguez-Arnold, J., Zhang, A., Cheng, S. Z. D., Lovinger, A. J., Hsieh, E. T., Chu, P., Johnson, T. W., Honnell, K. G., Geerts, R. G., Palackal, S. J., Hawley, G. R. and Welch, M. B. *Polymer* 1994, **35**, 1884
15 Miller, R. L. and Seeley, E. G. *J. Polym. Sci., Polym. Phys. Edn* 1982, **20**, 2297
16 Clark, E. J. and Hoffman, J. D. *Macromolecules* 1984, **17**, 878
17 Hoffman, J. D., Frolen, L. J., Ross, G. S. and Lauritzen Jr, J. I. *J. Res. Natl Bur. Stand.* 1975, **79A**, 671
18 Hoffman, J. D., Davis, G. T. and Lauritzen Jr, J. I. in 'Treatise on Solid-State Chemistry' (Ed. N. B. Hannay), Vol. 3, Plenum Press, New York, 1976, Ch. 7
19 Roitman, D. B., Marand, H., Miller, R. L. and Hoffman, J. D. *J. Phys. Chem.* 1989, **93**, 6919
20 Janimak, J. J., Cheng, S. Z. D., Giusti, P. A. and Hsieh, E. T. *Macromolecules* 1991, **24**, 2253
21 Point, J. J., Damman, P. and Janimak, J. J. *Polymer* 1993, **34**, 3771
22 Lauritzen Jr, J. I. and Hoffman, J. D. *J. App. Phys.* 1973, **44**, 4340
23 Lauritzen Jr, J. I. *J. Appl. Phys.* 1973, **44**, 4340
24 Hoffman, J. D., Guttman, C. M. and DiMarzio, E. A. *Faraday Discuss. Chem. Soc.* 1979, **68**, 177
25 Hoffman, J. D. *Polymer* 1982, **23**, 656
26 Hoffman, J. D. *Polymer* 1983, **24**, 3
27 Hoffman, J. D. and Miller, R. L. *Macromolecules* 1988, **21**, 3038
28 Lovinger, A. J. personal communication, 1993
29 Lovinger, A. J. *Bull. Am. Phys. Soc.* 1994, **39**, 107